A Switched Gain Resonant Controller to Minimize Image Artifacts in Intermittent Contact Mode Atomic Force Microscopy

Matthew W. Fairbairn and S. O. Reza Moheimani, *Fellow, IEEE*

***Abstract*—As the scan speed of the atomic force microscope (AFM) operating in intermittent contact mode is increased, the likelihood of artifacts appearing in the image is increased due to the probe tip losing contact with the sample. This paper presents an analysis of the effects of probe loss and a new method, switched gain resonant control, of reducing the problem of probe loss when imaging at high speed. The switched gain resonant controller is implemented to switch the cantilever quality *Q* factor according to the sample profile during the scan. If the controller detects that the probe has lost contact with the sample the cantilever *Q* factor is increased leading to a faster response of the feedback controller, expediting the resumption of contact. A significant reduction in image artifacts due to probe loss is observed when this control technique is employed at high scan speeds.**

***Index Terms*—Atomic Force Microscopy, field-programmable analog array (FPAA), quality factor control, resonant control.**

I. Introduction

THE atomic force microscope (AFM) [1] generates 3-D images of a sample surface by scanning the sample underneath a cantilever with a sharp probe tip and measuring the change in cantilever displacement due to the variations of the sample topography. Simply dragging the sample underneath the cantilever in constant contact (contact mode) may result in damage to soft or delicate samples and samples which are weakly attached to a substrate. When operating in intermittent contact mode [2], [3] the probe tip intermittently contacts the sample rather than dragging across it. Intermittent contact mode is the preferred mode of AFM imaging for many applications as the lateral forces (friction) exerted by the tip on the sample are significantly reduced. It is also an advantage to use intermittent contact mode on hard samples as lateral forces in contact mode may lead to excessive wearing of the tip. A worn (blunt) tip leads to reduced image resolution.

In intermittent contact mode, the microcantilever is oscillated at a fixed frequency, close to its first resonant mode with an amplitude of 10–100 nm, lightly tapping the sample once every oscillation cycle. The tip actuation force is commonly provided by applying a sinusoidal signal to a piezoelectric actuator located at the base of the cantilever or a thin film of piezoelectric material deposited on the surface of the cantilever.

As the sample is scanned underneath the cantilever, variations in the sample height modify the force between the tip and the sample. This change in force between the tip and sample modifies the effective damping factor and resonance frequency of the cantilever [2], [4], [5]. As the slope and peak of the resonance curve is modified, the oscillation amplitude of the cantilever will also change. This change in oscillation amplitude of the cantilever is proportional to the change in sample height.

The force exerted by the tip on the sample may be high enough to damage the sample/tip or distort the image due to compression of the sample when an abrupt increase in the sample height is encountered. For the case when a reduction in sample height is encountered, the tip may lose contact with the sample.

To reduce the forces between the tip and the sample and to allow improved tracking of large sample features, a feedback control loop is employed to regulate tip–sample force by moving the sample stage in the vertical (*Z*) direction. This feedback loop is illustrated by the block diagram of Fig. 1. By maintaining the cantilever oscillation amplitude $A(t)$ at a constant value $A_{\rm set}$ the feedback loop maintains a constant tip–sample force.

The optical lever method [6] is the most common means of measuring the cantilever displacement. A laser beam is reflected off the surface of the cantilever onto a split photodiode sensor. Movement of the reflected beam on the photodiode sensor is proportional to cantilever tip displacement. To recover the tip oscillation amplitude $A(t)$, the signal provided by the photodiode sensor is demodulated by a lock in amplifier or RMS to dc converter to remove the sinusoidal excitation signal.

$A(t)$ is then subtracted from $A_{\rm set}$ to provide the error signal for the *Z*-axis feedback controller. The most popular form of *Z*-axis feedback controller in commercial AFMs is a PI controller. The advantage of the PI controller is that it is relatively easy to tune as the cantilever parameters and sample type/environment are varied.

The *Z*-axis actuator which moves the sample stage in the vertical direction is commonly incorporated into a piezoelectric tube scanner which is used to scan the sample laterally in the *X*- and *Y*-axis as well. The *Z*-axis controller must compensate for changes in the oscillation amplitude, due to variations in sample height, by sending an appropriate signal to the *Z*-axis actuator. The controller output is therefore proportional to the

Manuscript received May 28, 2012; revised August 16, 2012; accepted August 21, 2012. Date of publication August 31, 2012; date of current version November 16, 2012. This work was supported by the Australian Research Council. The review of this paper was arranged by Associate Editor M. De Vittorio.

The authors are with the School of Electrical Engineering and Computer Science, The University of Newcastle, Callaghan, N.S.W. 2308, Australia (e-mail: matthew.fairbairn@newcastle.edu.au; Reza.Moheimani@newcastle.edu.au).

Color versions of one or more of the figures in this paper are available online at http://ieeexplore.ieee.org.

Digital Object Identifier 10.1109/TNANO.2012.2216288

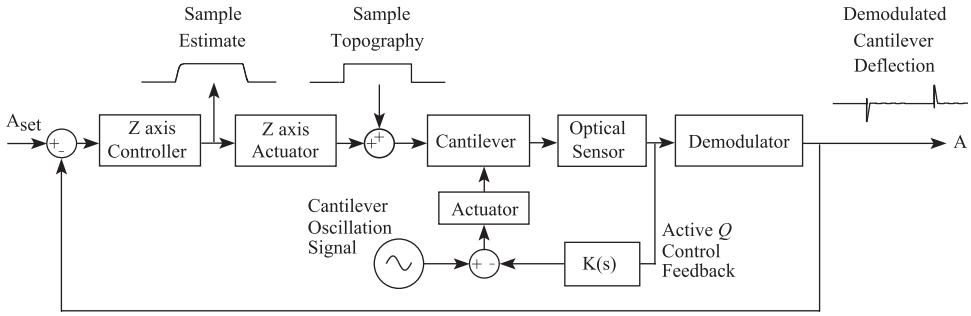

Fig. 1. Block diagram of the *Z*-axis feedback control loop used to maintain a constant cantilever oscillation amplitude and estimate the sample height as the sample is scanned under the cantilever. An optional active *Q* control feedback loop is also shown.

sample topography as the sample is scanned underneath the cantilever. The controller output at each lateral coordinate is processed by a computer to form a 3-D image of the sample. As the oscillation amplitude is regulated, the probe tip should track the sample topography. The faster the feedback loop is able to track the topography the more accurate the estimate of sample topography is.

One hindrance of the AFM operating in intermittent contact mode is its relatively slow scan speed. In some applications, it may be desirable to increase the scan speed to increase productivity. One example is defect detection in electronic grade silicon devices [7]. A high scan speed may be required to capture dynamic processes, an example of this would be biological processes [8] which occur in the range of milliseconds. Commercially available AFMs are too slow to observe such processes as they may take up to a minute to image one frame of a biological sample.

The main constraint to scan speed is the bandwidth of the *Z*-axis feedback loop. A high bandwidth feedback loop will allow for a large *Z*-axis controller gain. Increasing the *Z*-axis controller gain will result in a faster response speed of the *Z*-axis actuator leading to better tracking and a more accurate estimate of sample topography. The gain of the *Z*-axis controller is limited by the stability margins of the feedback loop.

In free air, the cantilever may be modeled by the second-order transfer function

$$G(s) = \frac{D(s)}{V(s)} = \frac{\beta\omega_n^2}{s^2 + 2\zeta\omega_n s + \omega_n^2} \tag{1}$$

where $D(s)$ is cantilever displacement, $V(s)$ is the oscillation voltage, β is the steady-state gain, and ζ $\left(\zeta = \frac{1}{2Q}\right)$ is the damping factor of the cantilever.

When the tip is interacting with the sample, the dynamics of the cantilever are modified due to the influence of the tip–sample force F_{TS}. Variations in F_{TS} cause a shift in ω_n and ζ. It is important that significant stability margins are maintained to accommodate for these deviations in parameters as the sample is scanned below the cantilever. If the loop bandwidth is too low instabilities will appear in the sample image as the scan speed is increased.

The two main limitations to the stability margins are the transient response time of the cantilever and the time taken to demodulate the oscillation amplitude.

The cantilever in cascade with the RMS to dc converter/lock in amplifier resembles a first-order transfer function with a bandwidth of $\sigma = \frac{\omega_n}{2Q}$ [9]. It takes several periods of oscillation before an accurate measure of $A(t)$ is produced by a demodulation system such as the RMS to dc converter or lock in amplifier. This results in a delay in the error signal and controller response. The *Z*-axis actuator typically has a much higher bandwidth than the cantilever/demodulator transfer function, so for this analysis the *Z*-axis actuator transfer function may be assumed to be a unity gain. If the controller is an integrator with a transfer function $C_I(s) = \frac{K_Z}{s}$, the simplified open loop transfer function of the *Z*-axis feedback loop becomes

$$\frac{K_Z}{s}\frac{\beta e^{-T_D s}}{\left(\frac{s}{\sigma}+1\right)} \tag{2}$$

where T_D is the demodulation delay. The stability margins of the loop will therefore depend on K_Z, β, T_D, and σ. Reducing T_D and/or increasing σ will result in an increase in the stability margins of the loop allowing for an increase in K_Z to provide for faster tracking of sample features.

σ may be increased by increasing ω_n [10], [11] or reducing Q [12]. ω_n is increased by reducing the size of the cantilever. This, however, may reduce the ability of the probe to track large sample changes. Q may be reduced artificially through the use of active Q control [9]. A high Q is required for high force sensitivity/image resolution [13]. However, most commercial AFM cantilevers have a much higher Q factor than is needed for the desired image resolution when scanning samples in air.

One other factor which also affects scan speed is the set point amplitude of oscillation A_{set}. It is important that F_{TS} be kept to a minimum to reduce image distortion from sample compression and to avoid tip/sample damage.

The average force between the cantilever tip and the sample [14] is given by [15], [16]

$$F_{\mathrm{TS}} \propto \frac{k}{Q}\sqrt{(A_0^2 - A_{\mathrm{set}}^2)} \tag{3}$$

where k is the spring constant of the cantilever and A_0 is the free air oscillation amplitude of the cantilever. F_{TS} may be reduced by increasing Q or A_{set}. When imaging soft delicate samples, it is common to set A_{set} at 80–90% of A_0 to minimize F_{TS}. This high value of A_{set} may limit the maximum achievable scan speed if the sample contains abrupt variations in height.

If the image being scanned has a sharp deep drop in topography, it is possible that the cantilever tip will lose contact with the sample for some period of time. This phenomenon is commonly referred to as "parachuting" or "probe loss." As the probe tip is not interacting with the sample, the resulting signal provides no information about the sample topography. The image artifacts due to probe loss are worsened as $A_{\rm set}$ and the scan speed are increased. If the drop in topography is large enough error signal saturation is likely to occur which will increase the duration of probe loss.

When probe loss occurs, it is desirable that the error signal sent to the feedback controller be as large as possible so that the controller brings the sample back in contact with the probe tip in as short a time as possible. A high value for $A_{\rm set}$ may be a limitation on downhill slopes of the sample as it limits the magnitude of the maximum error signal ($e_{\max} = |A_{\rm set} - A_0|$), which increases the probability of error signal saturation occurring [12], [17]. A high value for $A_{\rm set}$, however, is an advantage when imaging uphill regions of the sample as it allows for a larger value for the maximum error signal ($e_{\max} = A_{\rm set}$) presented to the Z-axis feedback controller. A controller which compensates the error signal on steep downhill regions to allow for a high value of $A_{\rm set}$ will give significant benefits such as an increased maximum error signal in upward regions of topography and reduced tip–sample force.

The switched gain resonant controller introduced in this article addresses the problem of probe loss, reducing image artifacts at high scan speeds while minimizing tip–sample forces.

II. Analysis of Imaging Artifacts Due to a Large Steep Drop in Sample Topography

In this section, an analysis of the artifacts which occur due to probe loss when $A_{\rm set}$ is set close to A_0 is presented. A scan over a vertical step drop in sample topography is depicted in Fig. 2 as a "worst case" scenario.

Before point *a* is reached on the sample shown in Fig. 2, the probe is scanning a flat surface and oscillating at $A(t) = A_{\rm set}$. At point *a,* the probe encounters the sharp drop in topography and detaches from the sample. This causes $A(t)$ to increase exponentially according to the relationship [12]

$$A(t) = A_{\rm set} + (A_0 - A_{\rm set})\left(1 - e^{\frac{-\omega_n}{2Q}t}\right) \tag{4}$$

where the time t begins at zero from the edge of the step. During this transient time, the error signal is smaller than the change in sample topography. This low error signal will delay the speed of response of the *Z*-axis feedback controller to bring the sample back in contact with the probe tip. The length of this transient depends on the cantilever *Q* factor and ω_n.

The feedback error signal does not respond to the change in $A(t)$ immediately due to the delay in demodulating the cantilever displacement signal. The controller output will be delayed as a result of this. This delay occurs between points *a* and *b* in Fig. 2.

At point *b,* the controller output begins to reflect this exponential increase of $A(t)$. The amplitude $A(t)$ will continue to increase until $A(t) = A_0$. At point *c,* in the diagram the cantilever has reached its free air oscillation amplitude A_0. Another delay occurs due to demodulation before this is reflected in the control signal at point *d*.

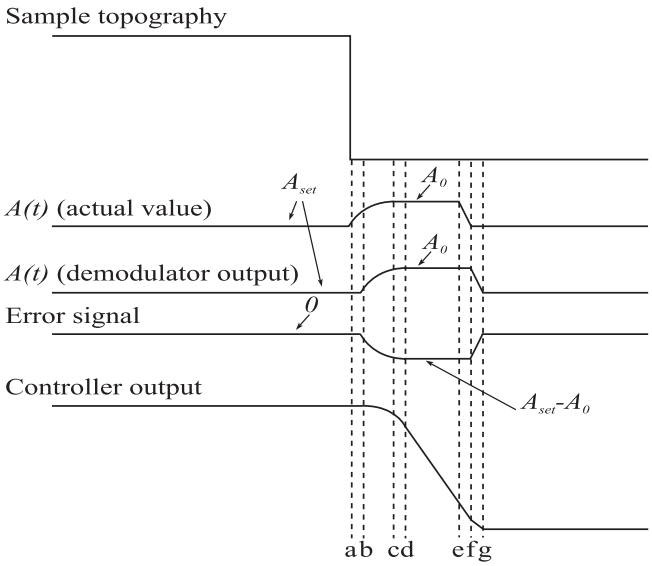

Fig. 2. High-speed scan of a sample with a sharp downward step. The tapping amplitude is limited to A_0 after the step is encountered. This causes the error signal to saturate limiting the speed of the feedback loop.

At point *d,* the magnitude of the error signal has saturated and is limited to $e_{\max} = |A_{\rm set} - A_0|$. The relatively small magnitude of $e_{\max}$ constrains the *Z*-axis feedback loop to a slow response causing the cantilever to oscillate in free air with an amplitude of A_0 until the *Z*-axis actuator can bring the sample back into contact with the probe. This slow response prolongs the time that the probe is detached from the sample.

When the probe tip is not in contact with the sample the controller output will not be an accurate representation of the sample topography. When the error signal is saturated, the integral action in the feedback controller will cause the sample topography to appear linear with a slope proportional to the controller gain and the value of $e_{\max}$, and inversely proportional to the scan speed. This can be seen in the region between points *d* and *e* in Fig. 2.

At point *f,* the probe regains contact with the sample. This is reflected in the control output at point g.

III. Methods of Reducing Imaging Artifacts Due to a Sharp Drop in Sample Topography

The image artifacts due to probe loss are affected by the scan speed, feedback controller gain and the value of $e_{\max}$. These parameters are fixed for the duration of a scan. Several researchers have shown that by modifying these parameters dynamically, according to the profile of the sample, significant improvements in image quality at high scan speeds can be achieved. These strategies all involve some form of detection to determine whether the probe is detached from the sample and a switching controller dependent on the detection signal.

A. Reducing Scan Speed

When the probe encounters a step drop of height Δh, the duration that the probe is detached from the sample depends on Δh, the *Z*-axis feedback controller gain and $e_{\max}$. If the scan speed is reduced, a smaller area of the sample will be scanned during this period of probe loss reducing the affected area. In most cases, however, a high scan speed is desirable. Otero *et al.* [18] developed a feedforward controller which controls the scan speed depending on the predicted sample topography. If a region of the sample topography is predicted to be flat by the controller then the scan speed would be set at a high rate. If a drop in the sample topography is encountered, the rate of change in the oscillation amplitude would signal to the controller that a downward slope was about to occur and the scan speed would be reduced by the controller.

B. Increasing the Controller Gain

The *Z*-axis controller gain and cantilever *Q* factor must be chosen to ensure that sufficient stability margins are achieved for the *Z*-axis feedback loop. This will avoid oscillations appearing in the image due to loop instability. If the stability margins are widened this will allow for an increase in the controller gain to reduce the duration of probe loss.

Artificially reducing the cantilever *Q* factor results in an increase in bandwidth of the *Z*-axis feedback loop allowing a higher controller gain to be used. This may be achieved by the use of active *Q* control, which uses velocity feedback to modify the effective cantilever *Q* factor. This method reduces the probe loss time [12] at the cost of increased tapping forces.

When the tip has lost contact with the sample the problem of high tip–sample force and oscillations from instability is not present. This means that when the tip is off-sample the controller gain may be set higher than the maximum gain allowable for on-sample stability. Momentarily increasing the controller gain, to increase the *Z* feedback response speed, when the tip is off-sample will reduce or eliminate error signal saturation without induced instability in the feedback loop. The controller gain must be reduced back to the appropriate on-sample value when the tip regains contact with sample to avoid large tip– sample forces and instabilities in the feedback loop.

Kodera *et al.* [19] approached the error saturation problem using a dynamic PID *Z*-axis feedback controller. The signal $A(t)$ is used to determine whether the probe tip has detached from the sample or not. If $A(t)$ exceeds a threshold value A_{thresh} (set close to A_0), then it is inferred that the cantilever has lost contact with the sample. When probe loss is detected the error signal $(A_{\text{set}} - A_0)$ is multiplied by a gain before it is sent to the controller. This has the effect of increasing the actuator's response speed and reducing the time that the probe is detached from the sample surface. When the probe regains contact with the sample $A(t)$ quickly falls below the threshold value, and the gain is removed from the error signal avoiding any instabilities.

De *et al.* [20] developed the reliability index method to determine if the tip has lost contact with the sample, rather than using the measured value of $A(t)$. To obtain the reliability index, an observer is designed to model the dynamics of the cantilever in free air. The reliability index is the error between the observer model and the cantilever. When the tip interacts with the sample the forces between the tip and sample modify the effective stiffness and damping of the cantilever. The on-sample cantilever dynamics will therefore be different to the observer model which is based on the cantilever oscillating in free air. When the cantilever is operating in free air the reliability index should be small and increase when the tip is tapping the sample, giving an indication of when the probe has lost contact with the sample. Agarwal *et al.* [21] used a switched gain PID controller with a threshold value of the reliability index determining the switching between gains to reduce the problem of error saturation.

The authors in [22] combined the approaches of switching scan speed and feedback gain with good results. Their control philosophy involved reducing the scan speed in uphill regions of the sample to allow for a higher on-sample feedback gain and switching the feedback gain when probe loss is detected on downward sloping regions of the sample.

C. Increasing the Maximum Error Signal

The duration of probe loss may be reduced by increasing $e_{\max}$ which for downward slopes of the sample can be achieved by setting A_{set} much lower than A_0. The disadvantage of doing this is that F_{TS} will be increased according to (3) and $e_{\max}$ on upward slopes of the sample will be reduced.

For a cantilever oscillating in free air near its resonance frequency the amplitude of oscillation is proportional to the cantilever Q factor. This means that $e_{\max}$ may be increased by increasing the cantilever *Q* factor.

When the probe is on-sample, the *Q* factor should be set at a value low enough to maintain sufficient stability margins in the *Z*-axis feedback loop. A_{set} should be set close to A_0 to minimize F_{TS} and increase $e_{\max}$ in upward sloping regions of the sample. When the probe is off-sample instabilities appearing in the image are no longer an issue. Therefore, the *Q* factor may be increased in this region to increase A_0 (and consequently $e_{\max}$) to reduce the probe loss duration.

Gunev *et al.* [23] introduced a controller which switches the *Q* factor of the probe depending on the profile of the sample. The controller uses the principle of active *Q* control, multiplying probe velocity by a gain *G* and subtracting it from the probe oscillation signal, to set the on-sample cantilever *Q* factor. If the oscillation amplitude of the probe exceeds a threshold value A_{thresh} the gain *G* is reduced, which increases the *Q* factor. As the probe comes back into close proximity with the sample the forces between the tip and the sample will modify the *Q* factor and resonance frequency of the cantilever causing $A(t)$ to return below A_{thresh}. As $A(t)$ is now less than A_{thresh} the controller increases G back to its on-sample value which has the effect of reducing *Q* to ensure that the stability margins on the loop are wide enough to avoid instabilities appearing in the image.

Gunev *et al.* demonstrated that the use of this control philosophy results in a significant reduction of imaging artifacts caused by probe loss while maintaining a high value for A_{set} to limit tip–sample forces and maintain a high value for $e_{\max}$ in

upward sloping regions of the sample. However, the techniques that Gunev *et al.* used to implement this control philosophy do not allow for easy implementation into existing commercial AFMs. The AFM used by Gunev *et al.* to demonstrate adaptive *Q* control was a custom-made device which used a laser Doppler vibrometer to measure the cantilever velocity. This velocity signal was used in the active *Q* control feedback loop to modify the cantilever *Q* factor. The cantilever displacement signal used to track the sample topography was obtained by integrating the velocity signal.

The switched gain resonant controller presented in this study is based on the control philosophy of switching the cantilever *Q* factor to a high value, when probe loss is detected, to increase the feedback response speed in regions where the probe has detached from the sample. This new controller uses a resonant controller, which uses the tip displacement signal for feedback, to modify the cantilever *Q* factor. Therefore, it may be easily integrated into existing commercial AFMs which are not typically fitted with a velocity sensor. This new controller is designed to be compact, simple to modify control parameters, and limit the effects of noise in the feedback loop.

IV. Active *Q* Control With Resonant Control Velocity Feedback

The active *Q* control loop incorporated inside the *Z*-axis feedback loop is shown in Fig. 1. The cantilever tip velocity signal is required for feedback when modifying the effective cantilever *Q* factor with active *Q* control. Commercial AFMs are typically fitted with a displacement sensor to measure variations in the sample topography. Incorporating a velocity sensor to the system would be difficult and costly. It is therefore common to estimate the velocity signal from the displacement signal. In Fig. 1, the controller $K(s)$ estimates the velocity and applies a gain to obtain the desired effective cantilever *Q* factor.

A differentiator may be used to estimate tip velocity from the displacement signal; however, a differentiator amplifies high-frequency sensor noise in the feedback loop. Most commercial applications of active *Q* control use time delay of the probe displacement signal to estimate probe velocity. Adding a delay of $\frac{3\pi}{2}$ radians to the sinusoidal displacement signal at the oscillation frequency provides an estimate of the tip velocity.

Using the time delay method to estimate tip velocity presents a risk of exciting higher order unmodeled resonant modes of the cantilever due to spill-over effects [24]. This may lead to a degradation of system performance or instability [25].

A new method of tip velocity estimation for use in active *Q* control was introduced by Fairbairn and Moheimani [26]. Using this technique a resonant controller [27] approximates a differentiator in a narrow band of frequencies, applying a gain at only these frequencies. This controller eliminates amplification of high-frequency noise by a differentiator and ensures that unmodeled cantilever dynamics are not excited by the control action.

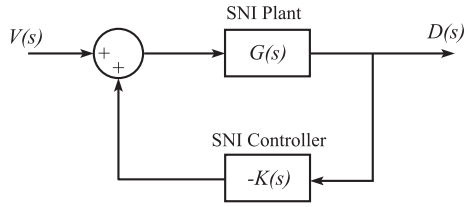

Fig. 3. Resonant control feedback loop arranged in a positive feedback context. The cantilever model $G(s)$ and controller $-K(s)$ both have strictly negative imaginary transfer functions.

The transfer function of the resonant controller used in this study to modify the effective cantilever *Q* factor is

$$K(s) = \frac{\alpha s^2}{s^2 + 2\zeta_c \omega_n s + \omega_n^2} \tag{5}$$

where α and ζ_c are control design parameters which determine the gain at the frequency of interest ω_n and the bandwidth of control.

The resonant controller is implemented in the active *Q* control feedback loop shown in Fig. 1. The input to this feedback loop is the voltage $V(s)$ which is applied to the actuator that oscillates the cantilever and the output is the cantilever displacement $D(s)$ measured by the photodiode sensor.

To analyze the stability of the resonant control feedback loop in the presence of unmodeled cantilever dynamics the feedback loop may be rearranged as a positive feedback loop by multiplying the controller $K(s)$ by -1, as shown in Fig. 3, and applying negative imaginary systems theory [28], [29]. An alternate proof is given in [30] and [31].

A transfer function whose Nyquist plot for $\omega \geq 0$ lies on or below the real axis is defined as negative imaginary (NI). If the Nyquist plot of a negative imaginary transfer function does not touch the real axis, except for at $\omega = 0$, the transfer function is defined as strictly negative imaginary (SNI). $-K(s)$ and $G(s)$ are SNI, even when higher order modes are included in the model of $G(s)$.

The condition for guaranteed stability in the presence of unmodeled dynamics when two NI transfer functions are connected in a positive feedback loop is that at least one of the transfer functions must be SNI and the dc loop gain is less than one [28]. The resonant control feedback loop of Fig. 3 satisfies both criteria.

The closed-loop transfer function of the resonant control feedback loop is

$$T(s) = \frac{D(s)}{V(s)} = \frac{G(s)}{1 + G(s)K(s)}. \tag{6}$$

The desired *Q* factor may be obtained by placing the poles of $T(s)$ at desired locations using a pole placement optimization technique [26]. The *Q* factor may then be tuned by varying the gain of the controller α. Increasing α results in a decrease in the cantilever *Q* factor, and vice versa.

V. Switched Gain Resonant Controller

In this section, a new method of implementing the control philosophy described in Section III-C is presented. The switched

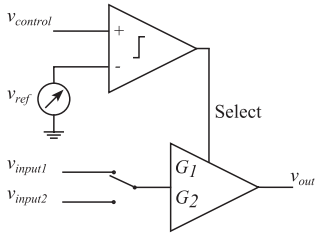

Fig. 4. Anadigm comparator with a switchable input CAM.

gain resonant controller detects probe loss from a threshold value of $A(t)$ and modifies the cantilever Q factor between a low value and a high value depending whether the tip is on or off-sample. The switched gain resonant controller, shown in Fig. 5, replaces $K(s)$ in the active Q control feedback loop of Fig. 1.

A field programmable analog array (FPAA) [32] was used to implement this controller as it allows for the controller parameters to be easily modified to accommodate for changing cantilever parameters and environmental conditions. FPAAs consist of configurable arrays of switched capacitor operational amplifier circuits which may be configured to implement transfer functions via computer interface software. The FPAA and interface circuitry (electronics to convert the single ended signals from the AFM to differential signals used by the FPAA as well as a summer for the feedback loop) occupy a small footprint which is an advantage when integrating the controller into an existing commercial AFM system.

A. Switch Implementation

The Anadigm AN220E04 FPAA [33] used in this study has many Configurable Analog Modules (CAMs) which may be configured using the Anadigm Designer2 interface software [33]. One such CAM is a comparator with a switchable gain which is used in the implementation of the switching controller. As shown in Fig. 4, the comparator selects the input to be passed through the gain stage according to the level of the input control signal $V_{\rm control}$. There are two possibilities for the value of the CAM output voltage $V_{\rm out}$:

$$V_{\rm out} = G_1 V_{\rm input1} \text{ if } V_{\rm control} < V_{\rm ref} \tag{7}$$

and

$$V_{\rm out} = G_2 V_{\rm input2} \text{ if } V_{\rm control} > V_{\rm ref}. \tag{8}$$

G_1 and G_2 are configurable gains and $V_{\rm ref}$ is a configurable reference voltage.

In this application, the value of $V_{\rm ref}$ is set to equal the threshold value of cantilever deflection amplitude $A_{\rm thresh}$. $V_{\rm control}$ is connected to the demodulated value of cantilever deflection *A(t)*.

The switched gain resonant controller which uses the comparator with switchable inputs CAM to limit error saturation is shown in Fig. 5. There are two modes of operation:

$$v_{\rm out} = K(s)G_1 \text{ if } A(t) < A_{\rm thresh} \tag{9}$$

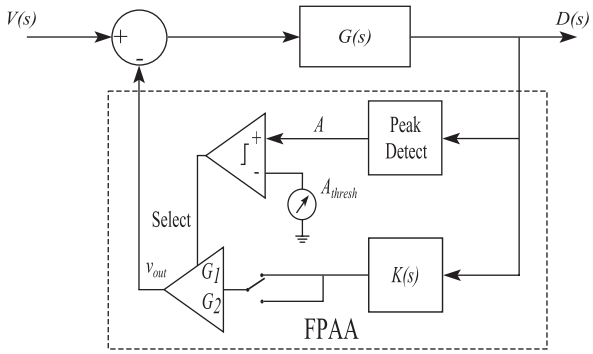

Fig. 5. Switched gain resonant control feedback loop. The blocks inside the dotted line are implemented in the FPAA.

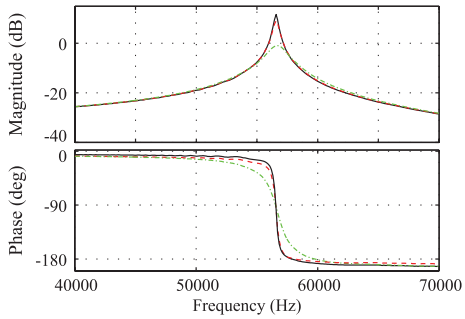

Fig. 6. Frequency response of the DMASP cantilever. Natural Frequency response, $f_r = 56\ 700$ Hz and $Q = 185$ (—). Frequency response with resonant active Q control, $Q = 50$ (- · -). Frequency response when probe is off-sample, $Q = 165$ (- -).

and

$$v_{\rm out} = K(s)G_2 \text{ if } A(t) > A_{\rm thresh} \tag{10}$$

where $K(s)$ is given in (5).

The parameters of $K(s)$ are set to obtain the desired on-sample Q factor. As this is the desired on-sample Q factor G_1 is set to 1. The desired on-sample Q factor should be set at a low enough value for a wide *Z*-axis feedback loop bandwidth but high enough to give sufficient force sensitivity.

The off-sample Q factor is dependent on the value of G_2. $K(s)$ is multiplied by G_2 when $A > A_{\rm thresh}$. G_2 must therefore be set to a value less than 1 to increase the cantilever Q factor when probe loss is detected.

B. Amplitude Demodulation

As the switched gain resonant controller uses the value of $A(t)$ to determine when the probe has detached from the sample it is important that $A(t)$ be measured accurately in as short a time as possible.

The methods used to demodulate the cantilever deflection signal such as the RMS to dc converter or lock in amplifier typically take approximately ten oscillation cycles to acquire an accurate measure of the demodulated signal [34]. This delay in measuring $A(t)$ may be significant when trying to minimize probe loss.

For a cantilever with a resonance frequency of 55 kHz, a delay of up to $\approx 180\ \mu$s would be expected to obtain an accurate

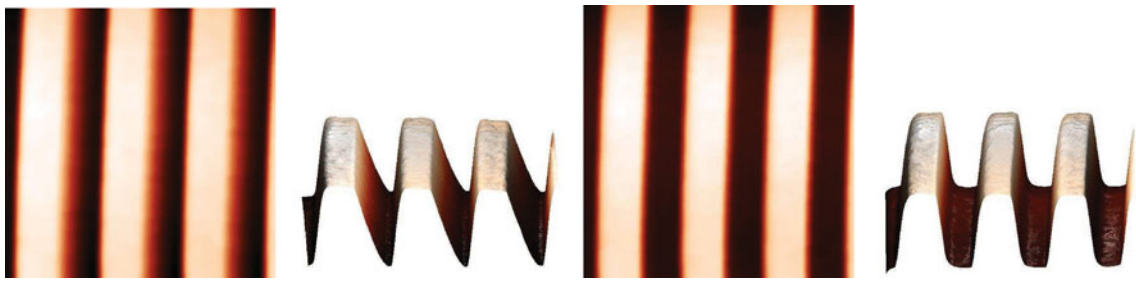

Fig. 7. Images of the NT-MDT TGZ1 calibration grating obtained at a scan speed of 40 μm/s. The use of the switching resonant controller resulted in significant reduction of probe loss as can be seen by the sharper downslope in the image. (a) 2-D image with Q control. (b) 3-D image with Q control. (c) 2-D image with switching resonant controller. (d) 3-D image with switching resonant controller.

measure of $A(t)$. At a scan rate of 40 μm/s, 7.2 nm of the sample would have been scanned laterally in this time.

Ando *et al.* [35] developed a much faster method of amplitude detection using sample hold circuits and a low pass filter to detect the peak of the sine wave and hold that value for a predefined time. This method enables accurate demodulation in up to half an oscillation cycle.

The peak detect CAM available in the Anadigm FPAA works in a similar manner to the demodulator developed by Ando *et al.* This CAM allows accurate measurements in less than one oscillation cycle. For the same cantilever with a resonance frequency of 55 kHz, the demodulation delay is less than $\approx$18 μs. At a scan rate of 40 μm/s, 0.72 nm of the sample would have been scanned laterally in this time.

Rather than using the demodulated displacement signal from the AFM to measure $A(t)$ for threshold amplitude detection a peak detect demodulator was implemented in the FPAA. The advantages of this are:

1) there are less input signals to connect to the controller making it easier to install in an existing AFM; and
2) it allows for faster detection of probe loss.

VI. Experimental Results

To demonstrate the improvements to scan speed and image reliability, when the switched gain resonant controller is employed in the AFM, experiments were conducted comparing images obtained with and without the controller.

The experiments were conducted with an NT-MDT NTEGRA AFM [36]. The NTEGRA AFM was fitted with a piezoelectric self-actuating AFM microcantilever, the Dimension Microactuated Silicon Probe (DMASP) manufactured by Bruker [37].

Images were obtained when the cantilever Q factor is dynamically modified by the switched controller and when the cantilever Q factor is set at a predefined value using active Q control.

An NT-MDT TGZ1 [36] periodic step calibration grating was used in this study as a test sample. The periodic step grating is ideal to test for probe loss as the sample shape and dimensions are known and it provides a worst case scenario. Step features such as these would be found on electronic devices such as integrated circuits. Characterization of such electronic devices is an application of the AFM where the scan speed is important to increase productivity. The NT-MDT TGZ1 calibration grating consists of a periodic step formed from silicon dioxide with a period of 3 $\pm$ 0.05μm and step height of 18.5 $\pm$ 1 nm. Images were obtained on a 10 μm $\times$ 10 μm section of the calibration grating at a scan speed of 40 μm/s. The free air cantilever oscillation amplitude was set to 53 nm with $A_{\text{set}} = 47$ nm, i.e., 89% of A_0. The Z-axis feedback controller is an integral controller with a gain K_Z. K_Z was increased until the loop became unstable. K_Z was then reduced slightly to ensure sufficient stability margins in the feedback loop. The same K_z was used for all scans.

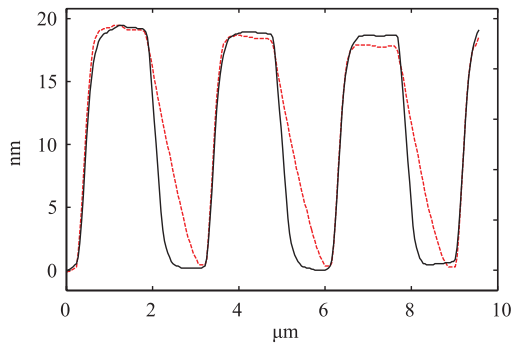

Fig. 8. Cross section of the NT-MDT TGZ1 sample topography obtained using active Q control (- -) and switched Q control (—).

The Q factor of the cantilever with no active Q control applied was measured to be 185. For the switched gain resonant controller the on-sample Q factor was set to 50 and the off-sample Q factor set to 165. Therefore, when the off-sample condition is detected the cantilever oscillation amplitude will increase by a factor of 3.3 which means that the maximum error sent to the feedback controller is magnified by this amount. A frequency response showing the cantilever response with no Q control, with the Q factor reduced to 50 and 165 is shown in Fig. 6. A_{thresh} was set to 51.5 nm i.e., 97% of A_0. To show the efficiency of the switched controller, scans obtained using active Q control (without switching) with the Q factor set to 50 which is the same as the on-sample Q factor used with the switched controller.

The resulting images obtained using only active Q control and using the switched gain resonant controller are shown in Fig. 7. A cross section of the images obtained is shown in Fig. 8.

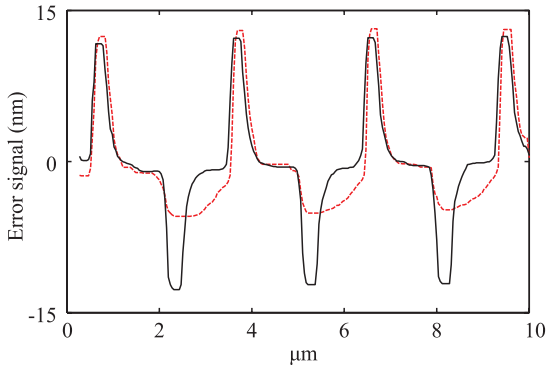

Fig. 9. Error signal for one scan line of the NT-MDT TGZ1 sample obtained using active Q control (- -) and switched Q control (—).

Significant probe loss can be observed in the image obtained using active Q control. This imaging artifact due to probe loss is signicantly reduced in the image obtained with the switched controller. The feedback error signal for the same cross section is shown in Fig. 9. Saturation of the error signal can be clearly seen in the image obtained with only active Q control.

It should be noted that a reduction in probe loss duration was observed in images obtained when the Q factor was reduced to 50 compared to images obtained with the unmodified Q factor of 185. With the same scan speed and a cantilever Q factor of 185 the maximum set-point obtainable was 65% of A_0. When $A_{\rm set}$ was increased to higher than 65% of A_0 the cantilever would completely detach from the sample and a flat image would be produced. Note that this sample has a large step drop. If a sample with smaller features was to be scanned at a lower scan speed then a higher set-point would be obtainable. If the Q factor had been reduced lower than 50 with active Q control the probe loss observed in Fig. 8 would be reduced. However, this may have detrimental effects such as reduced image resolution and increased tip–sample forces.

VII. Conclusion/Future Research

This study has highlighted the problem of imaging artifacts caused by probe loss when operating an AFM in intermittent contact mode. By setting the desired cantilever oscillation amplitude close to the free air amplitude tip–sample forces are minimized and tracking is improved in upward sloping regions of the sample. This high set point has a detrimental effect of increasing the likelihood of probe loss occurring in sharp downward sloping regions of the sample.

A switched gain resonant controller is presented in this study as a solution to this problem. When the probe loses contact with the sample the switched gain resonant controller increases the cantilever Q factor to increase A_0 which results in a faster feedback response. When the probe is off-sample A_0 may be much higher than $A_{\rm set}$ as tapping forces are irrelevant. The benefits of a high oscillation set point are therefore maintained while reducing the effects of probe loss. Increased imaging speeds with minimal image artifacts have been demonstrated using this control technique.

It takes some trial and error to determine the optimal values for $A_{\rm set}$, $A_{\rm thresh}$, the on-sample Q factor and the off-sample Q factor. Future research will look at automating the selection process of the aforeparameters, through an optimization process, to achieve increased scan speeds with minimal image artifacts and tip–sample force. Factors which would need to be considered are the cantilever properties, the sample type, the imaging environment and the height of the sample features.

Acknowledgment

The authors would like to thank Dr. A. Bazaei for his technical advice and the Australian Research Council for funding this research.

References

[1] G. Binnig, C. F. Quate, and C. Gerber, "Atomic force microscope," *Phys. Rev. Lett.*, vol. 56, no. 9, pp. 930–933, 1986.
[2] R. Garcia and R. Perez, "Dynamic atomic force microscopy methods," *Surf. Sci. Rep.*, vol. 47, no. 6–8, pp. 197–301, 2002.
[3] Q. Zhong, D. Inniss, K. Kjoller, and V. Elings, "Fractured polymer/silica fiber surface studied by tapping mode atomic force microscopy," *Surf. Sci.*, vol. 290, no. 1–2, pp. L688–L692, 1993.
[4] A. D. L. Humphris, J. Tamayo, and M. J. Miles, "Active quality factor control in liquids for force spectroscopy," *Langmuir*, vol. 16, no. 21, pp. 7891–7894, 2000.
[5] J. Tamayo, "Study of the noise of micromechanical oscillators under quality factor enhancement via driving force control," *J. Appl. Phys.*, vol. 97, no. 4, pp. 044903–044913, 2005.
[6] S. Alexander, L. Hellemans, O. Marti, J. Schneir, V. Elings, P. K. Hansma, M. Longmire, and J. Gurley, "An atomic-resolution atomic-force microscope implemented using an optical lever," *J. Appl. Phys.*, vol. 65, no. 1, pp. 164–167, 1989.
[7] G. Borionetti, A. Bazzali, and R. Orizio, "Atomic force microscopy: A powerful tool for surface defect and morphology inspection in semiconductor industry," *Eur. Phys. J. Appl. Phys.*, vol. 27, pp. 101–106, 2004.
[8] N. Kodera, D. Yamamoto, R. Ishikawa, and T. Ando, "Video imaging of walking myosin V by high-speed atomic force microscopy," *Nature*, vol. 468, pp. 72–76, 2010.
[9] J. Mertz, O. Marti, and J. Mlynek, "Regulation of a microcantilever response by force feedback," *Appl. Phys. Lett.*, vol. 62, pp. 2344–2346, May 1993.
[10] D. A. Walters, J. P. Cleveland, N. H. Thomson, P. K. Hansma, M. A. Wendman, G. Gurley, and V. Elings, "Short cantilevers for atomic force microscopy," *Rev. Sci. Instrum.*, vol. 67, no. 10, pp. 3583–3590, 1996.
[11] T. Ando, "High-speed atomic force microscopy coming of age," *Nanotechnology*, vol. 23, no. 6, pp. 062001–062006, 2012.
[12] T. Sulchek, G. G. Yaralioglu, C. F. Quate, and S. C. Minne, "Characterization and optimization of scan speed for tapping-mode atomic force microscopy," *Rev. Sci. Instrum.*, vol. 73, no. 8, pp. 2928–2936, Aug. 2002.
[13] B. Bhushan, *Springer Handbook of Nanotechnology*, (Gale Virtual Reference Library). New York: Springer-Verlag, 2006, vol. V. 2.
[14] R. D. Jaggi, A. Franco-Obregon, P. Studerus, and K. Ensslin, "Detailed analysis of forces influencing lateral resolution for Q-control and tapping mode," *Appl. Phys. Lett.*, vol. 79, no. 1, pp. 135–137, 2001.
[15] T. R. Rodriguez and R. Garcia, "Theory of Q control in atomic force microscopy," *Appl. Phys. Lett.*, vol. 82, no. 26, pp. 4821–4823, Jun. 2003.
[16] A. S. Paulo and R. Garcia, "Tip-surface forces, amplitude, and energy dissipation in amplitude-modulation (tapping mode) force microscopy," *Phys. Rev. B*, vol. 64, pp. 193411–193414, Oct. 2001.
[17] M. C. Strus, A. Raman, C.-S. Han, and C. V. Nguyen, "Imaging artefacts in atomic force microscopy with carbon nanotube tips," *Nanotechnology*, vol. 16, no. 11, pp. 2482–2492, 2005.
[18] J. Otero, H. Guerrero, L. Gonzalez, and M. Puig-Vidal, "A feedfordward adaptive controller to reduce the imaging time of large-sized biological samples with a SPM-based multiprobe station," *Sensors*, vol. 12, no. 1, pp. 686–703, 2012.

[19] N. Kodera, M. Sakashita, and T. Ando, "Dynamic proportional-integral-differential controller for high-speed atomic force microscopy," *Rev. Sci. Instrum.*, vol. 77, no. 8, pp. 083 704-1–083 704-7, Aug. 2006.
[20] T. De, P. Agarwal, D. R. Sahoo, and M. V. Salapaka, "Real-time detection of probe loss in atomic force microscopy," *Appl. Phys. Lett.*, vol. 89, no. 13, pp. 133119–133121, 2006.
[21] P. Agarwal, T. De, and M. V. Salapaka, "Real time reduction of probe-loss using switching gain controller for high speed atomic force microscopy," *Rev. Sci. Instrum.*, vol. 80, no. 10, pp. 103701–103705, 2009.
[22] A. Meshtcheryakov and V. Meshtcheryakov, "Scan speed control for tapping mode SPM," *Nanoscale Res. Lett.*, vol. 7, no. 1, pp. 121–125, 2012.
[23] I. Gunev, A. Varol, S. Karaman, and C. Basdogan, "Adaptive Q control for tapping-mode nanoscanning using a piezoactuated bimorph probe," *Rev. Sci. Instrum.*, vol. 78, no. 4, pp. 043 707–043 707-8, Apr. 2007.
[24] M. Balas, "Feedback control of flexible systems," *IEEE Trans. Autom. Control*, vol. 23, no. 4, pp. 673–679, Aug. 1978.
[25] R. Stark, "Time delay Q-control of the microcantilever in dynamic atomic force microscopy," in *Proc. 5th IEEE Conf. Nanotechnol.*, Jul. 2005, vol. 1, pp. 259–262.
[26] M. W. Fairbairn and S. O. R. Moheimani, "A new approach to active Q control of an atomic force microscope micro-cantilever operating in tapping mode," in *Proc. 50th IEEE Conf. Decis. Control*, Maui, Hawaii, Dec. 2012, pp. 259–262.
[27] H. R. Pota, S. O. R. Moheimani, and M. Smith, "Resonant controllers for smart structures," *Smart Mater. Struct.*, vol. 11, no. 1, pp. 1–8, 2002.
[28] I. Petersen and A. Lanzon, "Feedback control of negative-imaginary systems," *IEEE Control Syst.*, vol. 30, pp. 54–72, Oct. 2010.
[29] A. Lanzon and I. Petersen, "Stability robustness of a feedback interconnection of systems with negative imaginary frequency response," *IEEE Trans. Autom. Control*, vol. 53, no. 4, pp. 1042–1046, May 2008.
[30] D. Halim and S. O. R. Moheimani, "Spatial resonant control of flexible structures—Application to a piezoelectric laminate beam," *IEEE Trans. Control Syst. Technol.*, vol. 9, no. 1, pp. 37–53, Jan. 2001.
[31] S. O. R. Moheimani and B. J. G. Vautier, "Resonant control of structural vibration using charge-driven piezoelectric actuators," *IEEE Trans. Control Syst. Technol.*, vol. 13, no. 6, pp. 1021–1035, 2005.
[32] P. Gulak, "Field programmable analog arrays: Past, present and future perspectives," in *Proc. IEEE Region 10 Int. Conf. Microelectron. VLSI*, Nov. 1995, pp. 123–126.
[33] (2012). Anadigm dynamical programmable analog signal processing website. [Online]. Available: http://www.anadigm.com/an220e04.asp
[34] D. Abramovitch, "Low latency demodulation for atomic force microscopes, Part i efficient real-time integration," in *Proc. Amer. Control Conf.*, Jun. 29–Jul. 1, 2011, pp. 2252–2257.
[35] T. Ando, T. Uchihashi, and T. Fukuma, "High-speed atomic force microscopy for nano-visualization of dynamic biomolecular processes," *Prog. Surf. Sci.*, vol. 83, no. 79, pp. 337–437, 2008.
[36] (2012). NT-MDT website. [Online]. Available: http://www.ntmdt.com
[37] (2012). Bruker AFM probes website. [Online]. Available: http://www.brukerafmprobes.com/p-3252-dmasp.aspx

Matthew W. Fairbairn was born in Newcastle, Australia. He received the Bachelor's degree in electrical engineering from The University of Newcastle, N.S.W., Australia, in 2009, where he is currently working toward the Ph.D. degree in electrical engineering.

His research interests include the limitations of high-speed atomic force microscopy due to piezoelectric actuator and cantilever dynamics.

S. O. Reza Moheimani (F'11) received the Ph.D. degree in electrical engineering from Australian Defence Force Academy at the University of New South Wales, Canberra, Australia in 1996.

In 1997, he joined The University of Newcastle, N.S.W., Australia, in 1997, where he founded and directs the Laboratory for Dynamics and Control of Nanosystems, a multimillion-dollar state-of-the-art research facility dedicated to the advancement of nanotechnology through innovations in systems and control engineering. He is also a Professor and an Australian Research Council (ARC) Future Fellow with the School of Electrical Engineering and Computer Science, The University of Newcastle. His current research interests include mainly in the area of dynamics and control at the nanometer scale, and include applications of control and estimation in nanopositioning systems for high-speed scanning probe microscopy, modeling and control of microcantilever-based devices, control of electrostatic microactuators in microelectromechanical systems, and control issues related to ultrahigh-density probe-based data storage systems.

Prof. Moheimani is a Fellow of IFAC and a Fellow of the Institute of Physics (U.K.). He is a co-recipient of the 2007 IEEE TRANSACTIONS ON CONTROL SYSTEMS TECHNOLOGY Outstanding Paper Award, and the 2009 IEEE CSS Control Systems Technology Award, together with a group of researchers from IBM Zurich Research Labs, where he has held several visiting appointments. He has served on the editorial board of a number of journals including the IEEE TRANSACTIONS ON CONTROL SYSTEMS TECHNOLOGY, the IEEE/ASME TRANSACTIONS ON MECHATRONICS AND CONTROL ENGINEERING PRACTICE, and has chaired several international conferences and workshops.